Aeromagnetic Data Interpretation to Locate Buried Faults in South-East Cameroon

Theophile Ndougsa-Mbarga[1], Alain Narcisse S. Feumoe[2], Eliezer Manguelle-Dicoum[2] and James Derek Fairhead[3]*

[1] Department of Physics, Advanced Teacher's Training College, University of Yaoundé 1, P.O. Box 47, Yaoundé, Cameroon
[2] Department of Physics, Faculty of Science, University of Yaoundé I, PO Box 6052 Yaoundé, Cameroon.
[3] School of Earth and Environment, Faculty of Environment, University of Leeds, UK
* Corresponding author, theopndougsa@gmail.com/tndougsa@yahoo.fr

Abstract

The horizontal gradient and analytic signal techniques, and the 3-D Euler deconvolution have been applied to the aeromagnetic data from southeast Cameroon to delineate the subsurface structures. Determination of the magnitude maxima of: (1) the horizontal gradient of the total magnetic intensity field reduced to the equator (TMI-RTE), and (2) the analytic signal in addition to the main contacts deducted by Euler solution, allowed the production of a structural map showing the fault systems for the survey area. The suggested source depths are in the range of 600 to 6000 m. The deepest accidents are in NW-SE direction and have a depth of about 3000 to 4000 m in the southeast. On the other hand, the network of parallel major faults trending ENE-WSW have a shallow depth of about 1500 m. These major faults in the basement are associated to the Eburnean orogeny. These results reveal deep tectonic features, which up to date were unknown.

Keywords: Aeromagnetic, reduction to the equator, horizontal gradient, analytic signal, Euler deconvolution, upward continuation.

1. Introduction

The area under study is located in the southeastern part of Cameroon (Central Africa). This area was affected by a series of tectonic activities due to the collision between the Pan-African belt and the Congo craton that formed the structural features of the Southern Cameroon (e.g. *Nzenti et al.*, 1984 & 1988; *Castaing et al.*, 1994; *Abdelsalam et al.*, 2002; *Toteu et al.,* 2006). The collision resulted in the over thrusting of the Pan-African units onto the craton of about 50 to 150 km (*Nédelec et al.,* 1990; *Manguelle-Dicoum et al.,* 1992; *Tadjou et* al., 2009; *Shandini et al.,* 2010). Precambrian basement is deeply buried beneath the Pan-African formations across most of the study area. A major problem in this regard is that the regional structure and distribution of fault zones within the deeply buried Precambrian basement in southeastern Cameroon are currently not understood.

In the study area, the dense vegetation coverage does not permit direct geological studies and the determination of the subsurface structure of this region is fundamentally dependent on the use of regional geophysical surveys. In this paper, we attempt to remotely map the Precambrian basement structure using regional aeromagnetic survey data. Aeromagnetic data allow fast coverage of large and inaccessible areas for subsurface reconnaissance, which makes magnetic data analysis an essential tool of geophysical exploration. The processing of these data can provide important evidence for regional-scale basement faulting in southeastern Cameroon and thus for understanding the framework of the region. The principal objectives of this study are to demarcate the buried faults and to identify the important trends in the magnetic anomaly field.

2.   *Geologic and tectonic setting of study area*

Two structural domains can be distinguished in the study area (Fig. 1): the Yaoundé domain and the Ntem complex with its Proterozoic cover.
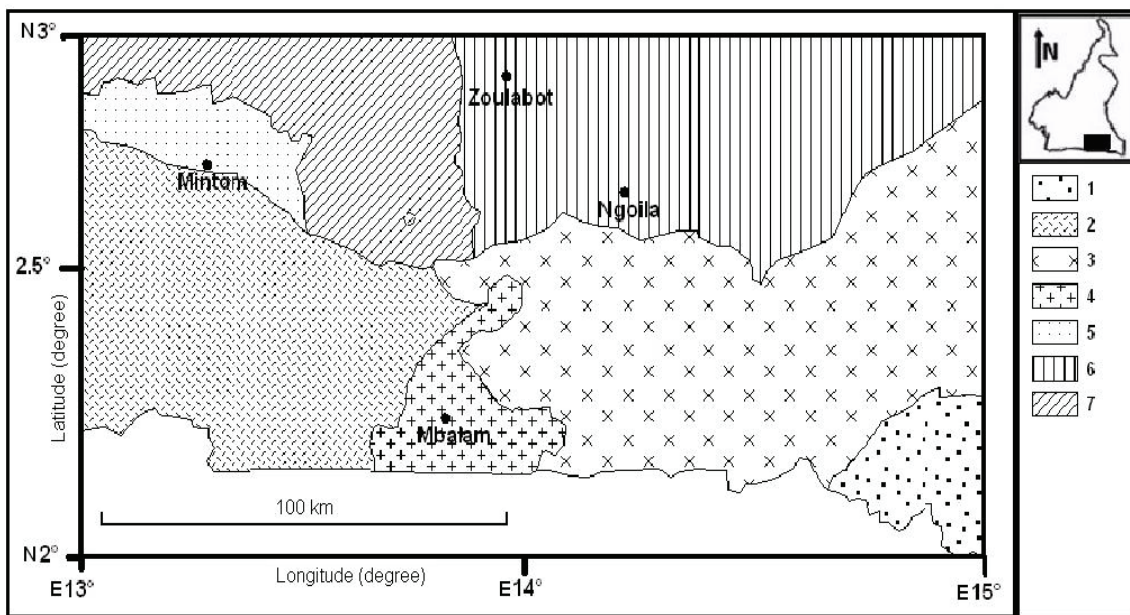

Fig. 1. Geological sketch map of the study area (modified after *Feybesse et al.,* 1987): 1 = Mouloundou tillite; 2 = Ntem unit; 3 = Lower Dja series; 4 = Mbalam series; 5 = Upper Dja series; 6 = Yokadouma series; 7 = Mbalmayo-Bengbis series.

The Yaoundé domain is a huge allochtonous nappe unit thrusted southward onto the Congo craton. This domain belongs to the Pan-African belt north and includes the Mbalmayo-Bengbis and Yokadouma series. It comprises low- to high-grade garnet-bearing schists, gneisses, and orthogneisses metamorphosed under a medium-to high-pressure metamorphism reaching the granulite facies.

The Ntem complex constitutes the northwestern part of the Congo craton and is very well exposed in southern Cameroon (*Maurizot et al.,* 1986). The complex is made up dominantly of Archean rocks with some reworked material that formed in Early

Proterozoic times (*Tchameni*, 1997). It includes Ntem unit and Mbalam series. The Pan-African units rest directly on the Ntem complex basement and constitute the second cover of the Congolese craton. The first craton cover (Proterozoic) is constituted by the Dja series and the tillitic complexes. It's discordant with the Mbalam belt and covered partially in the north by the Yaoundé nappe.

The major tectonic feature of the region is characterized by the extension of the Congo craton under the Pan-African units. This event marks the subduction of the Congolese craton under the Pan-African belt. The hypothesis of subduction of the Southern plate craton must have provoked deep fractures in covers. However, our knowledge about the buried faults in the area is rudimentary because of the paucity of geologic data. The present study deals with the application and correlation between geology and aeromagnetic data interpretation to establish the structural setting of the area under investigation.

3.   Materials and method

3.1   Aeromagnetic data

The key component of this study involved image enhancement of existing aeromagnetic datasets acquired by the company SURVAIR (contractor) for the CIDA (client) in 1970. Aeromagnetic surveys were flown with a flight height of 235 m and a nominal flight line spacing of 750 m in direction N°135. After correction of the measurements for the temporal variations of the magnetic field, the total magnetic intensity (TMI) anomaly was deduced by subtracting the theoretical geomagnetic field or IGRF (International Geomagnetic Reference Field) at each station. The TMI anomaly data were then upward continued to a height of a mean clearance of 1 km before they were merged into a unified digital grid, which has a cell size of 0.01 degree (i.e. 1.1 km). The reduction to the Equator method is applied. In this case, the magnetic field and magnetization will be horizontal as most of the magnetized sources. The Geosoft package software V 6.3 was used to reduce the field to equator (RTE) transformation of an anomaly in the Fourier domain. The inclination and declination angles of the ambient field were taken as -19.89 ° N and -5.88 °E, respectively (2.5°N, 14°E) in the center of the region at the date of January 1970 according to IGRF. A grid-based processing was made using GETECH's GET grid software.

The TMI map (Fig. 2) is characterized by high magnetic anomalies of ENE-WSW trending direction. This configuration may be attributed to relatively deep-seated low relief basement structures.

3.2   Methods

For the purpose of this study, several interpretation methods were applied with the final goal of enhancing the signature of hidden faults. The estimation of the locations of the magnetic contacts, associated with faults and other structural discontinuities was achieved by the application of horizontal gradient and analytic signal techniques. The

upward continuation height used is 2 km. It is not the same as the 1 km upward continuation height mentioned before in the initial data. Before using two analysis techniques we applied upward continuation to the gridded data. Upward continuation is an analytical transform that yields the response of a magnetic source body at given elevation above the original flight datum (*Telford et al.,* 1990). The transform attenuates high frequency signal components associated with shallow magnetic sources and tends to emphasize deep, regional-scale magnetic anomalies. Finally, in order to estimate source depths from gridded aeromagnetic data we applied the 3-D Euler deconvolution method. The theory and advantages of the different methods used are briefly discussed in sections below.
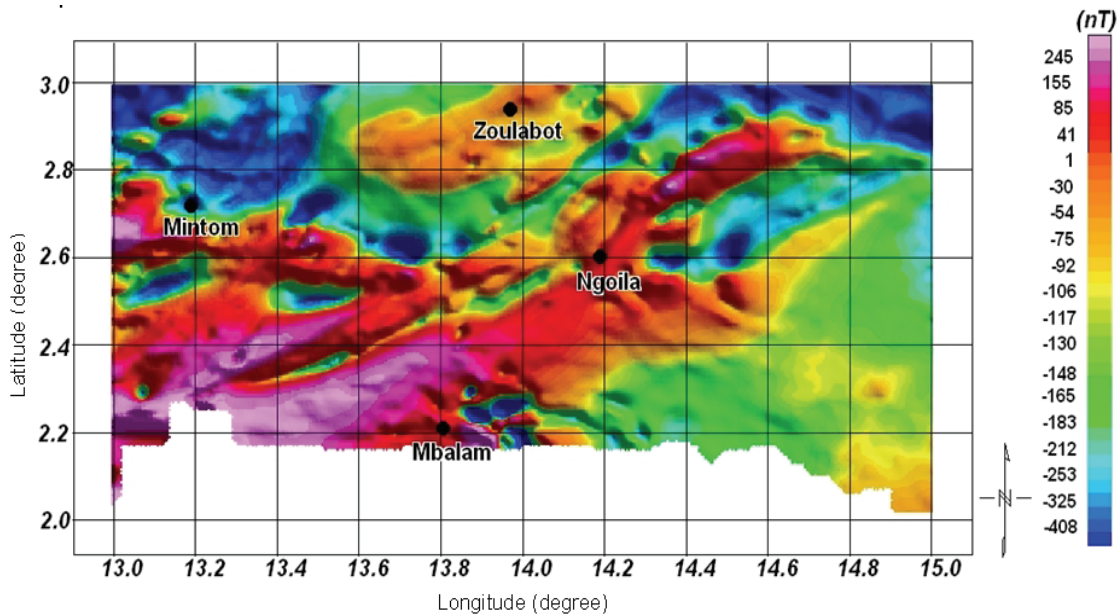

Fig. 2. Total magnetic intensity anomaly map of the study area (TMI).

3.2.1 Horizontal Gradient Method

The horizontal gradient method is in many ways the simplest approach to estimate contact locations of the bodies at depths. The biggest advantage of the horizontal gradient method is its low sensitivity to the noise in the data because it only requires calculations of the two first-order horizontal derivatives of the field (*Phillips,* 1998). If *M* is the magnetic field then the horizontal gradient magnitude (HGM) is given by:

$$HGM(x,y) = \sqrt{\left(\frac{\partial M}{\partial x}\right)^2 + \left(\frac{\partial M}{\partial y}\right)^2} \tag{1}$$

This function gives a peak anomaly above magnetic contacts under the following assumptions (*Phillips,* 1998): (1) the regional magnetic field is vertical, (2) the magnetizations are vertical, (3) the contacts are vertical, (4) the contacts are isolated, and (5) the sources are thick. Violations of the first four assumptions can lead to shifts

of the peaks away from the contacts. Violations of the fifth assumption can lead to secondary peaks parallel to the contacts. In order to partially satisfy the first two assumptions, it is usually necessary to perform a standard phase shift operation known as Reduction-to-Pole (RTP) on the observed magnetic field. In magnetic equatorial regions where inclination is less than 15°, RTP is generally unstable and cannot be derived. A similar effect is seen when a magnetic field is Reduced-to-Equator (RTE) instead of to the pole values as given above. Once the field has been reduced to the equator, the regional magnetic field will be horizontal and most of the source magnetizations will be horizontal (Fig. 3). Crests in the horizontal gradient magnitude grid can be located by passing a small 3 by 3 window over the HGM grid and searching for maxima (*Blakely and Simpson,* 1986).
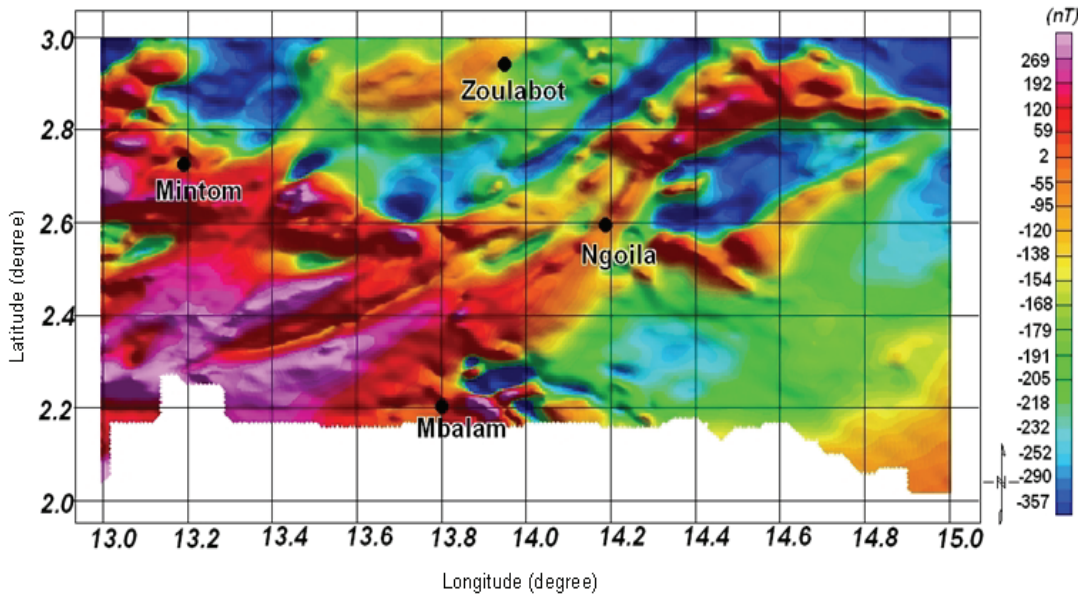

Fig. 3. Total magnetic intensity map reduced to the equator (TMI-RTE).

3.2.2   *Analytic Signal Method*

Absolute analytic signal magnitude (ASM) according to (*Nabighian,* 1972; *Roest et al.,* 1992; *MacLeod et al.,* 1993) can be defined as the square root of the squared sum of the vertical and horizontal derivatives of the magnetic field as:

$$\left| ASM(x,y) \right| = \sqrt{\left(\frac{\partial M}{\partial x} \right)^2 + \left(\frac{\partial M}{\partial y} \right)^2 + \left(\frac{\partial M}{\partial z} \right)^2} \tag{2}$$

The advantage of this method of magnetic data enhancement is that its amplitude function is always positive and does not need any assumption of the direction of body magnetization (*Jeng et al.,* 2003). In a manner identical to that used in the horizontal gradient method, peaks in the analytic signal amplitude are located. The maxima of the

analytic signal can be used to detect the structures responsible for the observed magnetic anomalies over the studied area.

3.2.3   3-D Euler Deconvolution Method

Depth estimation by Euler deconvolution technique was used for delineating geologic contacts. This technique provides automatic estimates of source location and depth. Therefore, Euler deconvolution is both a boundary finder and depth estimation method. Euler deconvolution is commonly employed in magnetic interpretation because it requires only a little prior knowledge about the magnetic source geometry, and more importantly, it requires no information about the magnetization vector (*Thompson,* 1982; *Reid et al.,* 1990).

Euler deconvolution is based on solving Euler's homogeneity equation (3) (*Reid et al.,* 1990):

$$(x-x_0)\frac{\partial M}{\partial x}+(y-y_0)\frac{\partial M}{\partial y}+(z-z_0)\frac{\partial M}{\partial z}=N(B-M) \tag{3}$$

where B is the regional value of the total magnetic field and (x_0,y_0,z_0) is the position of the magnetic source, which produces the total magnetic field M measured at (x,y,z). N is so called structural index. For each position of the moving window, on over-estimated system of linear equations is solved for the position and depth of the sources (*Thompson*, 1982; *Reid et al.,* 1990).

The most critical parameter in the Euler deconvolution is the structural index, N (*Thompson,* 1982). This is a homogeneity factor relating the magnetic field and its gradient components to the location of the source. Essentially, N measures the rate of change of the fields with distance from the source (fall-off-rate) and is directly related to the source dimensions. Therefore, by changing N, we can estimate the geometry and depth of the magnetic sources. A poor choice of the structural index has been shown to cause a diffuse solution of source locations and serious biases in depth estimation. Both *Thompson* (1982) and *Reid et al.* (1990) suggested that a correct N gives the tightest clustering of the Euler solutions around the geologic structure of interest. For magnetic data, physically plausible N values range from 0 to 3. The magnetic field of a point dipole falls off as the inverse cube, giving an index of 3, while an effective vertical line source such as a narrow, vertical pipe gives rise to an inverse square field fall-off and an index of 2. Values less than zero imply a field strength that increases with distance from the source (and is infinite at infinity).

4.   Results and interpretation

4.1   Contact locations

4.1.1   Analysis of the results of the horizontal gradient

The horizontal gradient method provides contact location that are continuous, thin and straight (Fig. 4a) compared on the TMI and RTE-TMI maps. The HGM map shows major anomalies in ENE-SWS and NE-SW directions. The amplitudes of gradient reaches 40nT/km. The anomalies correspond to a geological contact zone with a large magnetic susceptibility difference. In order to highlight the contacts direction shown on the HGM map, we show the maxima of the HGM map (Fig. 4b). This map reveals structural complexity such as faults inside the basement. For this reason, the horizontal
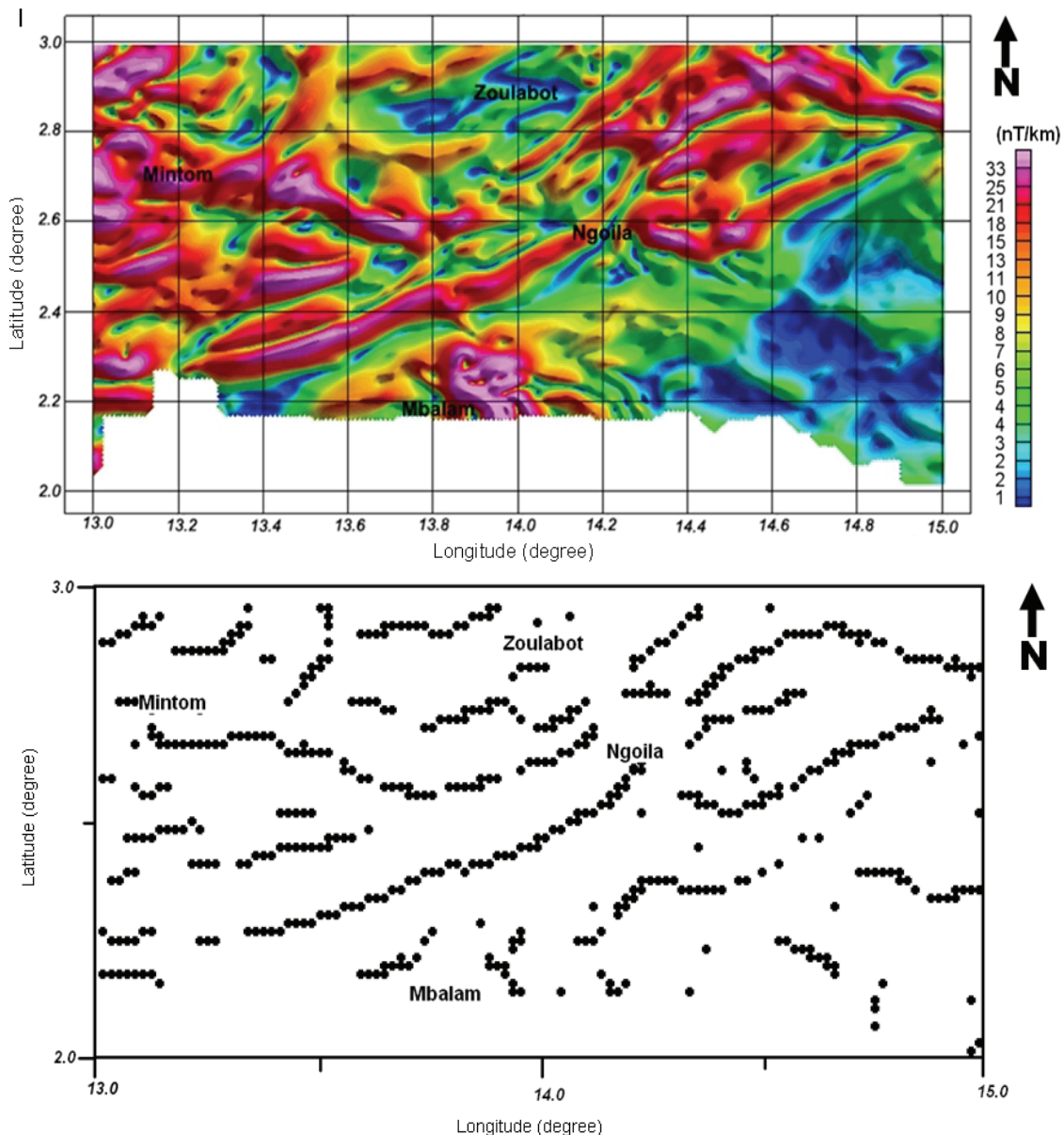

Fig. 4. a) Horizontal gradient magnitude of TMI- RTE map.
   b) Maxima of the horizontal gradient magnitude of the TMI-RTE.

gradient method is used to determine the locations of physical property (magnetization) boundaries. Two different structural domains were recognised within the survey area by differences in the inferred fault patterns, such as general orientation and spacing:

- The central domain characterized by major ENE-WSW and NE-SW direction. We can suppose that they affect the basement,

- The northwestern domain characterised by W-E trending lineaments.

Recall, however, that the horizontal gradient method requires many assumptions, and that violations of these assumptions can result in displacement of the contacts away from their true locations.

4.1.2   Analysis of the results of the Analytic Signal

The analytic signal method does not make the same assumptions, and does not result in displaced contacts. Based on these factors, the following criteria were used to interpret the final contact locations: (1) Where horizontal gradient contacts are isolated, they represent the best available contact location. (2) Where horizontal gradient contacts are parallel to and slightly offset from analytic signal contacts, the analytic signal contact represents the true contact location and the horizontal gradient contact indicates the down dip direction. As shown on the ASM map (Fig. 5), there are similarities between it and the HGM map (Fig. 4a). The locations of the maxima and the major shown ENE-WSW directions on the HGM map are represented also on the ASM map with high maximum amplitude of 50 nT/km.
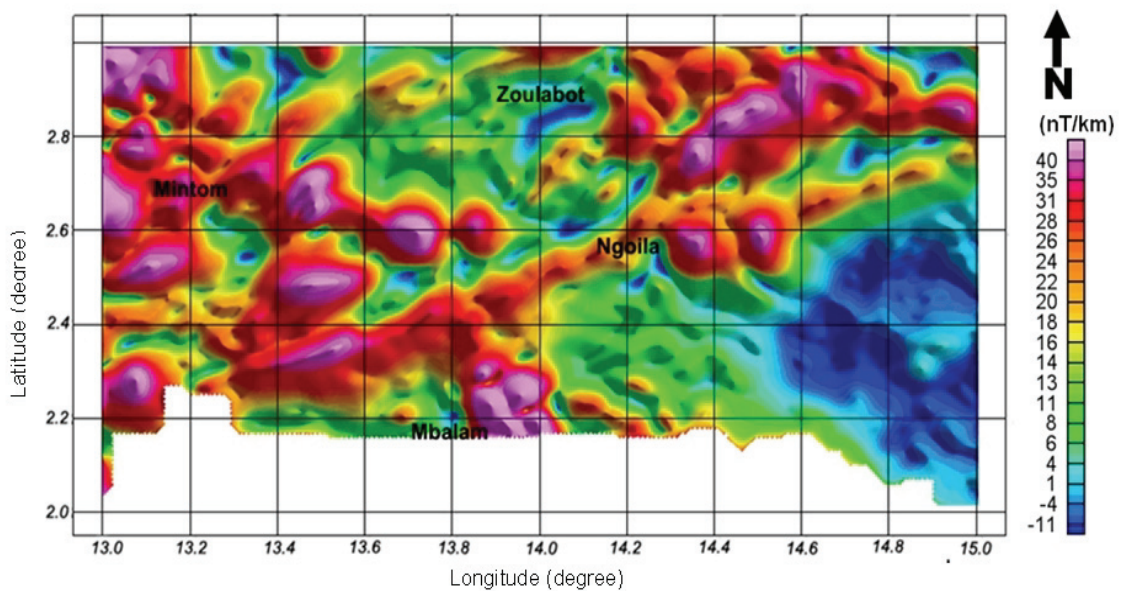

Fig. 5. Analytic signal magnitude of TMI-RTE map.

The two sets of contact locations resulting from the analysis of the magnetic map by horizontal gradient and analytic signal methods were combined as a colour composite image (Fig. 6).
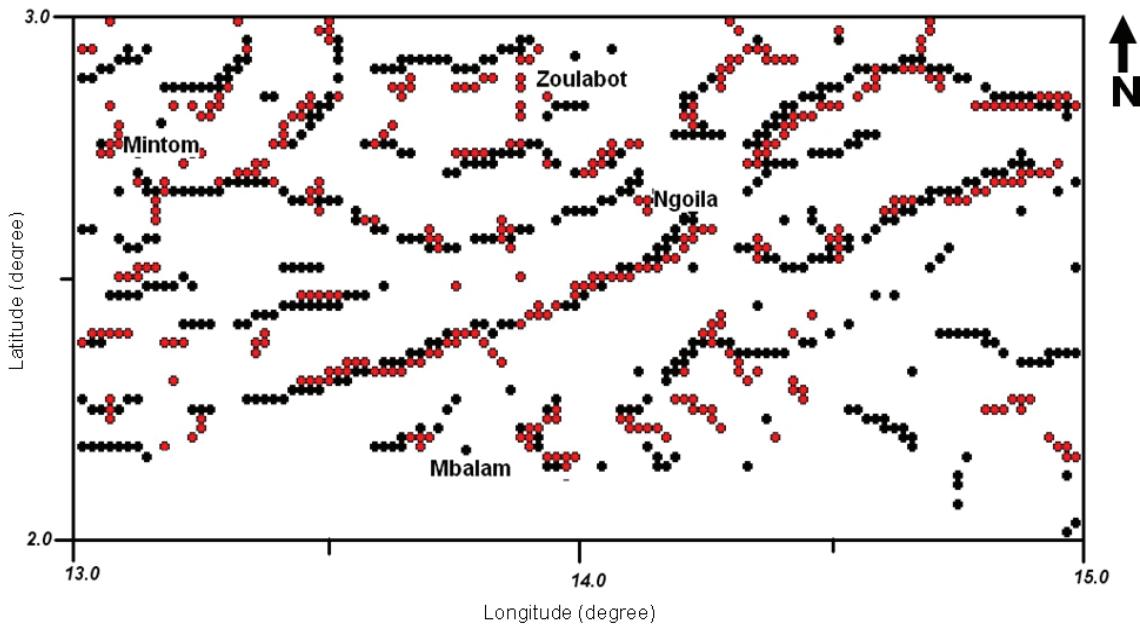

Fig. 6. Estimated locations of contacts according to the horizontal gradient method (black) and analytic signal method (red).

4.1.3   Contribution of the 3-D Euler deconvolution

The Euler method has been applied to the RTE-TMI map using a moving window of 20 km x 20 km. The Euler deconvolution was carried out on the study area using the Standard Euler 3D method of the Geosoft package software V.6.3. The Standard Euler 3D method is based on Euler's homogeneity equation that relates the magnetic field and its gradient components ($\frac{\partial M}{\partial x}, \frac{\partial M}{\partial y}$ and $\frac{\partial M}{\partial z}$ calculated in frequency domain) to the location of the source, with the structural index. The system uses a least squares method to solve Euler's equation simultaneously for each grid position within a window and then determines the anomaly position, depth, and base level for a specific magnetic source. We have assigned several structural index values and found that for a structural index of $N = 1.0$, the extension of linear clustering of Euler solutions given as coloured point (Fig. 7) shows the same main trends as the two previous methods. In addition, the Euler solution map reveals new deep contacts which accurate style trend in the southeast part of the area. The Euler plots in (Fig. 7) clearly define the solution for depths that range from 600 to 6000 m. Most of the Euler solutions in the centre show rather shallow depth of about 1500 m for the possible causative sources. The depths in the eastern part of the area are not uniform. In the north-eastern part, the solutions are situated at shallow depth with increasing depth, and in the south-eastern part the solutions are situated at deep depth of about 3 000 to 4 000 m. In the northwestern part

of the area, Euler plots also show non-uniform depth distribution from shallow to deep depths.
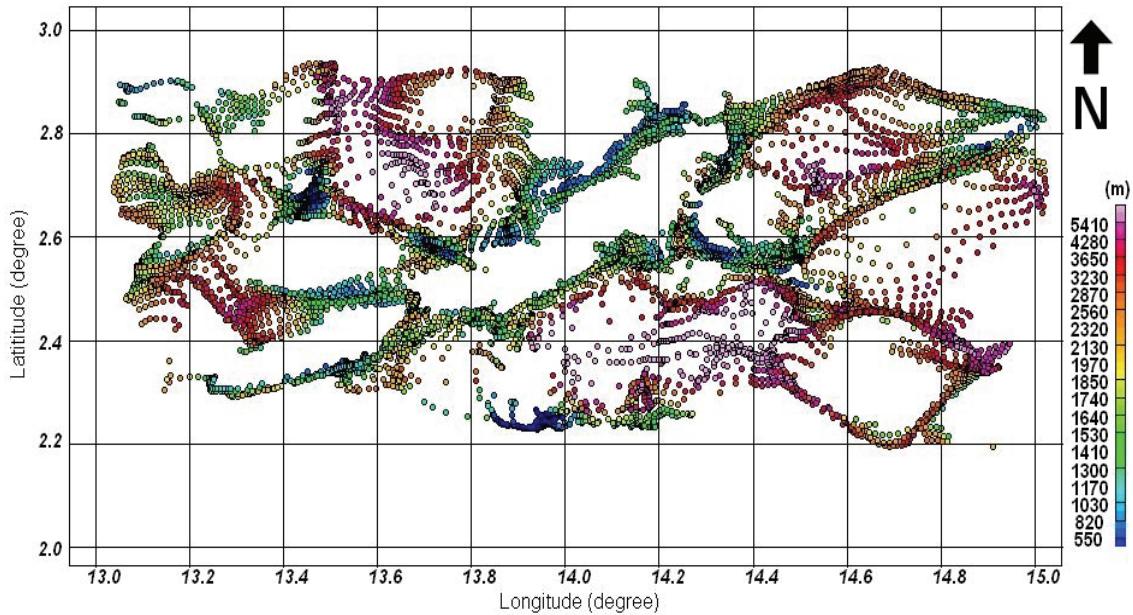

Fig. 7. Euler solution map for a structural index N=1.0, 2×2 km window and maximum relative error of 15%.

4.2   *Interpretation of the structural map of the study area obtained*

As discussed before, where horizontal gradient contacts are parallel to and slightly offset from analytic signal contacts, the analytic signal contact represents the true feature location and the horizontal gradient contact indicates the down dip direction. The observation of HGM and ASM maxima (Fig. 6) can thus be used to analyse dip directions of the faults; this information is even more visible in Euler solutions map. The Table 1. gives the characteristics of different fault segments and depths according to Euler solutions.

The three sets of contact locations resulting from the analysis of the magnetic data by horizontal gradient, analytic signal and Euler deconvolution methods were combined to aid in the final interpretation of contact locations. The combined map of structural zoning of the study area is shown in figure 8. Magnetic lineaments were traced by overlaying the maxima on the HGM and ASM map in addition to Euler solutions. Figure 8 shows the mapped faults superimposed on the geological map of the southeast Cameroon. The three major trends obtained from the analysis are:

(1)   The ENE-WSW and NE-SW trends are indicated by F_{16}, F_{15}, F_{12}, F_{21}, $F_{23,}$ F_{27} and some other minor lineaments.

(2)   The NW-SE and WNW-ESE trends are indicated by F_7, F_{26}, F_4, F_{11}, $F_{18,}$ F_{25} and other minor trends as shown on the map.

(3)   The E-W trend is represented by F_3, $F_{8,}$ and F_9.

Moreover, several minor magnetic trends are observed even though they have low frequency on the map.

Table 1. Characteristics of different fault segments and depths according to Euler solutions.

Fault segment	Dip	Depth (m)
F1	Vertical	1150
F2	WNW-ESE	1500
F3	N-S	1700
F4	Vertical	1500
F5	NNW-SSE	2500
F6	NW-SE	2500
F7	Vertical	5000
F8	N-S	
F9	Vertical	
F10	NW-SE	
F11	Vertical	4000
F12	N-S	1700
F13	NNW-SSE	
F14	NNW-SSE	
F15	Vertical	1700
F16	Vertical	1700
F17	NW-SE	1400
F18	Vertical	1600
F19	NW-SE	
F20	N-S	
F21	NW-SE	3000
F22	N-S	3000
F23	NW-SE	3000
F24	SW-NE	4000
F25	Vertical	4000
F26	Vertical	4000
F27	Vertical	4000

There is a tendency for all the faults to turn to a NE-SW and ENE-WSW direction, which correlate with the direction of subduction of the cratonic plate (Ntem complex) under the Pan-African. These major faults in the basement characterize the definitive stability of the Congo Craton and would be associated to the Eburnean orogeny. But several faults inferred from aeromagnetic anomalies in the southeastern part of the area turn to a NW-SE direction, indicating a significant change in fault geometry. The observed faults appear to cross-cut the Proterozoic Craton cover and therefore they should be post-dated, and the put in place of this reseau is in late Proterozoic.
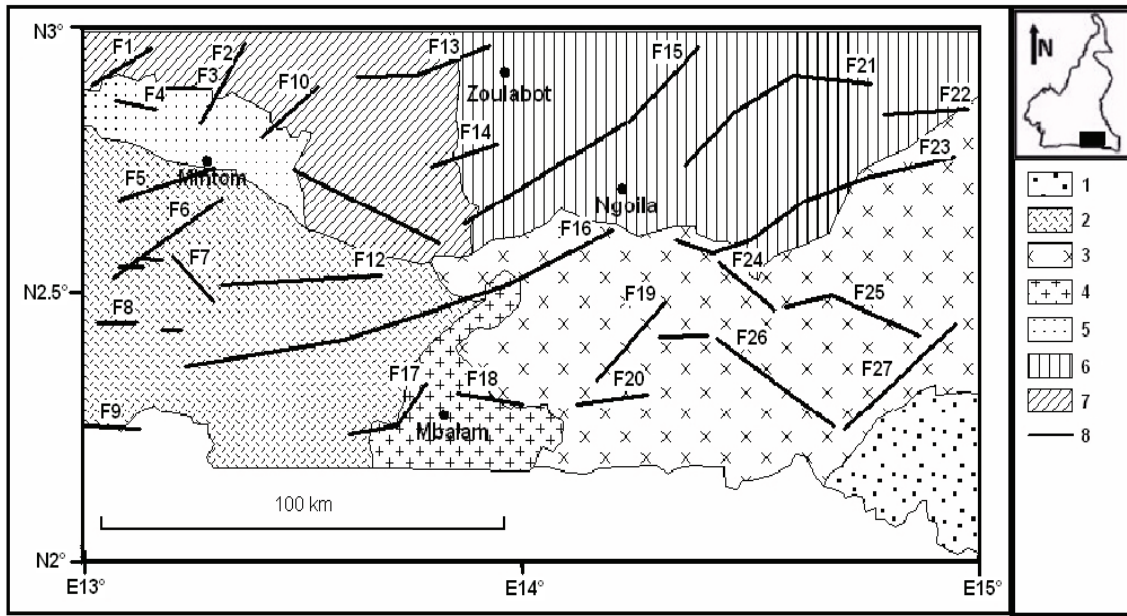
Fig. 8. Structural map of the study area. Interpreted contacts shown over a geological map. 1 = Mouloundou tillite; 2 = Ntem unit; 3 = Lower Dja series; 4 = Mbalam series; 5 = Upper Dja series; 6 = Yokadouma series; 7 = Mbalmayo-Bengbis series, 8 = Faults.

Aeromagnetic lineaments suggest that the area has been subjected to an important regional field stress. The predominant WSW-ENE and NE-SW fault trends affecting the area among which are faults F_{12}, F_{15}, F_{16}, F_{21} and F_{23} extend from southwest of the study area to the extreme northeast part. The regional field stress associated with the predominant trending of magnetic lineaments is in accordance with Eburnean orogeny trend (*Boukeke*, 1994) and would so have played an essential role in the control of the geodynamic evolution of the region. This regional stress fields affected the craton cover units in southeast Cameroon region and are responsible of the reorientation of the former structures (*Vicat*, 1998).

The application recently of the *multi-scale horizontal derivative of the vertical derivative* (MSHDVD) method (*Noutchogwe et al*, 2011) on the gravity anomaly map over the Foumban Shear Zone (FSZ) revealed the presence of a fault oriented N68°E and dipping towards southeast. According to *Noutchogwe et al.* (2011) this fault is hidden by volcanic formations, and it is linked to the ENE-WSW trending called Central African Shear Zone (CASZ), a dextral shear zone that extends some 2000 km from west Cameroon to Sudan (*Ngako et al.*, 2003; *Cornacchia and Dars*, 1983). It appears that, the reseau of faults identified in the area under study, with a major trend WSW-ENE to NE-SW is also connected to the CASZ.

5.   Conclusion

Filtering of magnetic data is used to enhance the data and to see features that would be difficult to detect without filtering. Application of selected filtering methods to the magnetic data of the southeastern Cameroon reveals the elements of subsurface structure in the study area. The structural map obtained for the area is dissected by many

faults, which have different directions indicating a complex tectonic history and several events of deformation. The major faults in the basement trend WSW-ENE to NE-SW and it is very likely that this stress field is associated to the Eburnean orogeny. It is found that, the faults identified in the area under study, with a major trend WSW-ENE to NE-SW are connected to the CASZ.

The structural and tectonic facts put in evidence are also in accordance with those discovered by some authors recently using gravity interpretation based on the *multi-scale horizontal derivative of the vertical derivative* (MSHDVD) method (*Noutchogwe et al*, 2011).

Acknowledgements

References

Abdelsalam, M.G., J.P. Liégeois and R.J. Stern, 2002. The Saharan metacraton. *Journal of African Earth Sciences*, **34**, 119–136.

Blakely, R.J. and R.W. Simpson, 1986. Approximating edges of source bodies from magnetic or gravity anomalies: *Geophysics,* **51**(7), 1494–1498.

Boukéké, D.B. 1994. Structures crustales d'Afrique centrale déduites des anomalies gravimétriques et magnétiques: le domaine précambrien de la République Centrafricaine et du Sud duCameroun. Thèse Doctorat, Université Paris Sud, Paris, France, 263 p.

Castaing, C., J.L. Feybesse, D. Thieblemont, C. Triboulet and P. Chevremont, 1994. Palaeogeographical reconstructions of the Pan,African/Brasiliano orogen: closure of an oceanic domain or intracontinental convergence between major blocks? *Precambrian Research*, **67**, 327–344.

Cornacchia, M. and R. Dars, 1983. Un trait structural majeur du continent africain. Les linéaments centrafricains du Cameroun au Golfe d'Aden. *Bull. Soc. Géol. France,* **25**, 101–109.

Feybesse, J.L., V. Johan, P. Maurizot and A. Abessolo, 1987. Evolution tectono-métamorphique libérienne et éburnéenne de la partie NW du craton zairois (SW Cameroun). In Current Research in African earth sciences, *Matheis & Schandelmeier* (eds), Balkema, Rotterdam, 9–13.

Jeng, Y., Y.L. Lee, C.Y. Chen and M.J. Lin, 2003. Integrated signal enhancements in magnetic investigation in archaeology. *Journal of Applied Geophysics*, **53**, 31–48.

MacLeod, I.N., K. Jones and T.F. Dai, 1993. 3-D analytic signal in the interpretation of total magnetic field data at low magnetic latitudes. *Exploration Geophysics,* **24**(4), 679–688.

Manguelle Dicoum, E., A.S. Bokosah and T.E. Kwende-Mbanwi, 1992. Geophysical evidence for a major Precambrian schist–granite boundary in southern Cameroon. *Tectonophysics*, **205***, 437–446.

Maurizot, P., A. Abessolo, J. Feybesse, L. Johan and P. Lecomte, 1986. Etude et prospection minière du Sud-Ouest du Cameroun : synthèse des travaux de 1978 à 1985. *Rapport BRGM 85 CMR 066*, 274 p.

Nabighian, M.N., 1972. The analytic signal of two-dimensional magnetic bodies with polygonal cross-section: its properties and use for automated anomaly interpretation. *Geophysics*, **37**(3), 507–517.

Nédélec, A., E.N. Nsifa and H. Martin, 1990. Major and trace element geochemistry of the Archaean Ntem plutonic complex South Cameroon: petrogenesis and crustal evolution. *Precambrian Research*, **47**, 35–50.

Ngako, V., P. Affaton, J.M. Nnange and T. Njanko, 2003. Pan-African tectonic evolution in central and southern Cameroon: transpression and transtension during sinistral shear movements. *Journal of African Earth Sciences*, **36**(3), 207–214.

Noutchogwe, T.C., C.T. Tabod, F. Koumetio and E. Manguelle-Dicoum, 2011. A gravity model study for differentiating vertical and dipping geological contacts with application to a Bouguer gravity anomaly over the Foumban Shear Zone, Cameroon. *Geophysica,* **47**(1–2), 43–55.

Nzenti, J.P., P. Barbey, J. Macaudière, and D. Soba, 1988. Origin and evolution of the late Precambrian high, grade Yaoundé gneisses Cameroon. *Precambrian Research*, **38**, 91–109.

Nzenti, J.P., P. Barbey, P. Jegouzo and C. Moreau, 1984. Un nouvel exemple de ceinture granulitique dans une chaîne protérozoïque de collision : les migmatites de Yaoundé au Cameroun. *Comptes Rendu de l'Académie des Sciences de Paris*, **299***, 1197–1199.

Phillips, J.D. 1998. Processing and Interpretation of Aeromagnetic Data for the Santa Cruz Basin - Patahonia Mountains Area, South-Central Arizona. U.S. *Geological Survey Open-File Report*, Arizona, 02–98.

Reid, A.B., J.M. Allsop, H. Granser, A.J. Millett and I.W. Somerton, 1990, Magnetic interpretation in three dimensions using Euler deconvolution. *Geophysics*, **55**, 80–90.

Roest, W.R., J. Verhoef and M. Pilkington, 1992. Magnetic interpretation using the 3-D analytic signal: *Geophysics,* **57**(1), 116–125.

Shandini, N.Y., J.M. Tadjou, C.T. Tabod and J.D. Fairhead, 2010. Gravity data interpretation in the northern edge of the Congo Craton, South-Cameroon. *Anuário do Instituto de Geociências*, **33**(1), 73–82.

Tadjou, J.M., R. Nouayou, J. Kamguia, H.L. Kande and E. Manguelle-Dicoum, 2009. Gravity analysis of the boundary between the Congo craton and the Pan,African belt of Cameroon. *Austrian Journal of Earth Sciences*, **102**(1), 71–79.

Tchameni, R., 1997. Géochimie et géochronologie des formations de l'archéen du paléoprotérozoïque du Sud Cameroun groupe du Ntem, Craton du Congo. Thèse de Doctorat, Université d'Orléans, Orléans, France, 186 p.

Telford, W.M., L.P. Geldard, R.E. Sherriff and D.A. Keys, 1990, Applied Geophysics. 2nd edition, Cambridge University Press, Cambridge, GB, 860 p.

Thompson, D.T., 1982. EULDPH: A new technique for making computer-assisted depth estimates from magnetic data. *Geophysics*, **47**, 31–37.

Toteu, S.F., R.Y. Fouateu, J. Penaye, J. Tchakounte, A.C.S. Mouangue, W.R. Van Schmuss, E. Deloule and H. Stendal, 2006. U-Pb dating of plutonic rocks involved in the nape tectonics in southern Cameroon: Consequence for the Pan-African orogenic evolution of the central African fold belt. *Journal of African Earth Sciences*, **44**, 479–49.

Vicat, J.P. 1998. Esquisse géologique du Cameroun : in Géosciences au Cameroun. *Collection GEOCAM,* 1/1998, 3–11.